MODEL PORES OF MOLECULAR DIMENSION

THE PREPARATION AND CHARACTERIZATION OF TRACK-ETCHED MEMBRANES

J. A. QUINN, J. L. ANDERSON, W. S. HO, *and* W. J. PETZNY

From the Department of Chemical Engineering, University of Illinois, Urbana, Illinois 61801. Dr. Quinn's present address is the School of Chemical Engineering, University of Pennsylvania, Philadelphia, Pennsylvania 19104. Dr. Anderson's present address is the School of Chemical Engineering, Cornell University, Ithaca, New York 14850. Dr. Ho's present address is the Corporate Research Laboratory, Allied Chemical Corporation, Morristown, New Jersey 07960. Dr. Petzny's present address is British Petroleum, Hamburg, West Germany.

ABSTRACT Extremely uniform pores of near molecular dimension can be formed by the irradiation-etching technique first demonstrated by Price and Walker. The technique has now been developed to the stage where it can be used to fabricate model membranes for examining the various steric, hydrodynamic, and electrodynamic phenomena encountered in transport through molecular-size pores. Methods for preparing and characterizing membranes with pores as small as 25 A (radius) are described in this paper. Results on pore size determination via Knudsen gas flow and electrolyte conduction are compared. Pore wall modification by monolayer deposition is also discussed.

INTRODUCTION

The analytical description of transport through porous membranes is not a straightforward problem. Compounding the theoretical treatment is the interdependence of chemical, electrical, and mechanical effects, each of which may contribute significantly to the flux through the membrane. Considerable progress has been made in treating macroscopic pores and, in the absence of a molecular theory, continuum descriptions valid for large pores are used to characterize pores of molecular dimension. As the size of the permeant, however, approaches that of the pore, a feature of most biological membranes, bulk fluid theories break down and effects due to finite solute and solvent size become dominant. The exact pore size below which continuum mechanisms are no longer valid is a subject of considerable discussion. Part of the controversy is due to the lack of reliable data on small pores. Biological membranes, as well as most synthetic membranes, do not have uniform, well-defined pores. In fact, pore dimensions must be deduced from the very equations whose validity is to be tested.

To cite one example of the type of problem encountered in modeling transport in pores of molecular dimension, consider the flux resulting from a pressure gradient imposed along the pore. It has been customary to apply hydrodynamic models derived for the motion of a sphere moving on the center line of a circular cylinder to describe the solute movement (1, 2). Such models, however, cannot adequately account for particle-wall interactions on a molecular level, nor do they allow for brownian motion which complicates the analysis by randomizing both position and orientation of the translating particle. The complexity mounts considerably if the particle and wall both have electrical charge, thereby introducing a host of interdependent electrokinetic phenomena.

Many of the problems involved in characterizing diffusion and "viscous flow" in biological membranes are discussed by Solomon (2). Bean (3) has recently published a comprehensive treatment of the physics of transport through porous membranes with a lucid discussion of the limitations of current theoretical models.

To test the various concepts and theories proposed for transport through pores and to explore the phenomena peculiar to molecular-sized pores, it is obvious that a well-defined, model membrane is required for experimental studies. Of the porous materials available it would appear that the model requirements are best fulfilled by membranes made by the track-etch process discovered by Price and Walker (4, 5) and subsequently developed by Bean (6, 7). The particularly desirable features of the track-etched pores formed in a thin sheet of, say, muscovite mica are: (*a*) pore density (number per square centimeter) and pore length can be accurately measured independently of any flux experiment; (*b*) pores as small as 25 A and as large as microns in radius can readily be formed; (*c*) all pores are oriented with axes perpendicular to the surface of the membrane; (*d*) all pores in any given membrane are identical with absolute pore radius measurable by several independent methods; (*e*) pores of large length-to-diameter ratio can readily be formed, minimizing end effects; (*f*) by monolayer coating techniques described in this paper, it is possible to control the chemical composition of the pore wall and to create pores with open radii less than 25 A, the approximate breakthrough radius resulting from the etching technique.

Track-etched mica membranes have been used in recent work of Bean and coworkers (6, 7) in studying convection and diffusion of water through pores as small as 150 A in radius and in electrolyte conductance studies of the etching process (7). Beck and Schultz (8) have used these membranes in an investigation of hindered diffusion; Anderson and Quinn (9) have measured the energy of activation for viscous momentum transport in dilute electrolyte solutions in track-etched pores as small as 56 A in radius; and Petzny and Quinn (10) have coated the pore walls of etched membranes with oriented layers of saturated fatty acids.

Since these membranes seem destined to play a prominent role in fundamental investigations of membrane transport and since many important steps in their

preparation and calibration have not been presented in the literature, it is our intention to summarize here those methods we have found to be successful in the preparation, cleaning, and characterization of track-etched membranes. We also include our results on pore wall modification by monolayer deposition.

To form these membranes a thin sheet of mica (or some other suitable insulating material) is exposed to massive fission fragments from a radioactive source. The resulting damage tracks in the irradiated sheet are etched into uniform pores by aqueous hydrofluoric acid. The physics of the track formation has received considerable attention (11–14) and Bean et al. (7) have proposed a theory for the etching process. In the sections below we outline our methods for sample preparation, for pore size determination, and for coating the pore walls.

MEMBRANE PREPARATION

Thickness Determination

Cleaved sheets of muscovite mica (15) are commercially available (Asheville-Schoonmaker Mica Company, Newport News, Va.). Starting with sheets 7–8 μ thick, with uncut area as large as 100 cm^2, several circular discs (3 cm) are cut with a sharp blade and template. The discs are cleaned with diethyl ether and weighed. Disc thickness is calculated from measured mass, area, and density (16). Thickness variation within a sheet is less than 0.5%.

Track Formation

A convenient fission fragment source is the radioisotope, californium-252. The apparatus used in irradiating mica discs with the ionizing particles emanating from an 0.2 μg ^{252}Cf source is shown in Fig. 1. The californium is electroplated onto a platinum strip which is fixed at the base of the chamber (a vacuum desiccator). Mounted above the source is an adjustable Plexiglas plate with a cylindrical stand holding the mica. An aluminum shield attached to a rotating solenoid switch normally covers the source; for irradiation, the switch is energized, the shield swings through a 30° angle leaving the source exposed.

The irradiation procedure is as follows: the disc is placed in a recess on the collimating stand, the desiccator is sealed, and the pressure lowered below 0.05 mm Hg. The solenoid is then energized for the desired irradiation time.

The irradiation rate ($\dot{n}$) of the source is calibrated by irradiating a disc for a fixed time (τ), etching the resulting tracks to a size large enough to be seen under a light microscope and counting the pore density (n): $\dot{n} = n/\tau$. Our half-life measurements on ^{252}Cf agree with the literature value, 2.55 yr (17). Since the distance between the source and disc (h) divided by the diameter of the irradiated region (d_0) is greater than 4, $\dot{n}$ is independent of d_0 ; also, $\dot{n}(h)$ drops off as h^{-2} (16). For this collimation ratio the tracks are normal to the membrane face, implying pore length is equal to membrane thickness.

Because partially penetrating, etched tracks appear identical with pores which traverse the entire membrane when viewed under an optical microscope, the calibration procedure described above actually measures the rate of impingement of heavy fragments at the exposed face of the membrane. To check for penetration, a second disc can be placed on top of the first and calibrated in the same manner. Our results indicate that only $\frac{1}{3}$ of the impinging fragments traverse a 7 μ membrane at 70 mm Hg and a collimation height of 8.9 cm, whereas essentially 100% pass through at 0.10 mm Hg. At high vacuum, fragments should be capable of traversing 10–12 μ of mica (12).

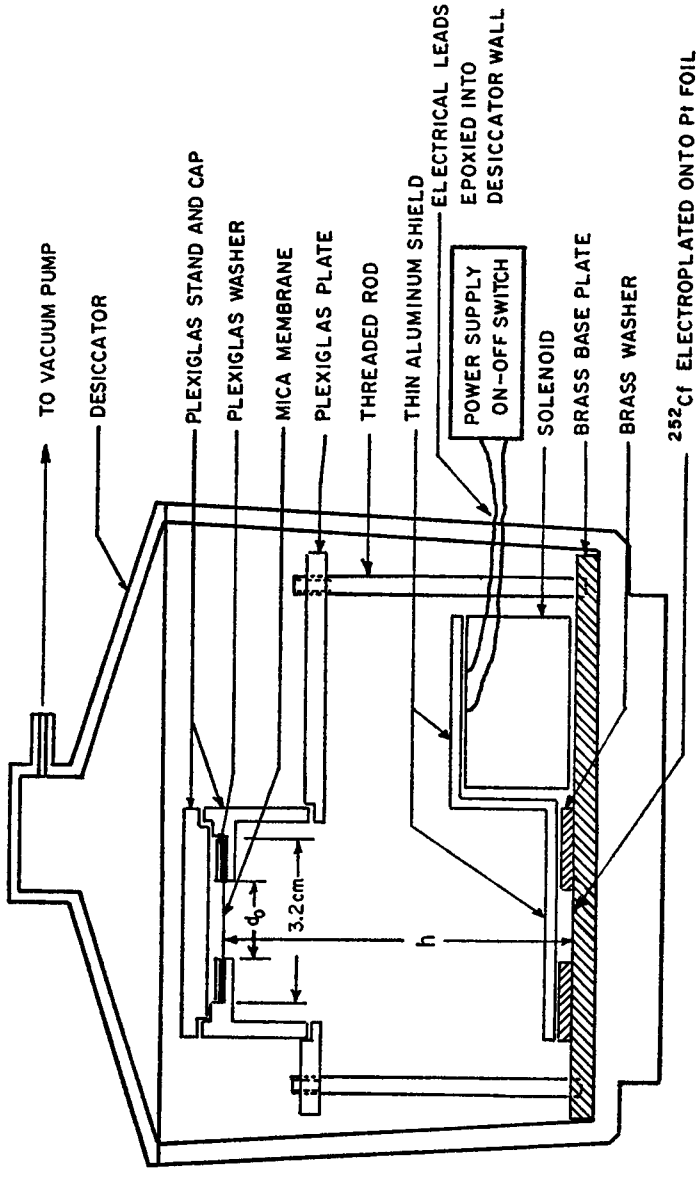

FIGURE 1 Irradiation apparatus for producing collimated damage tracks in thin sheets of mica. Fission fragment source is 0.2 μg of ^{252}Cf electroplated on platinum foil.

Track Etching

The damaged tracks are vulnerable to attack by hydrofluoric acid. Each track produces a single pore, while nondamaged regions of the mica remain unaltered. The etching process is initiated by placing the irradiated disc in a Nalgene cup and pouring aqueous HF onto it (time = 0). This cup floats on the surface of a water bath, thus maintaining temperature control. Etching is terminated by quenching the membrane with distilled water (time = t). The etched membrane is stored under chromic acid. Because the membrane is thin, the pore interior responds rapidly to conditions in the etching solution; a characteristic diffusion time is of the order of the square of the pore length divided by the diffusion coefficient of the acid, a time of some 0.05 sec for a 7 μ membrane. Mixing during the quenching step, however, may introduce an uncertainty of as much as 2 sec in the total etching time.

Etched pores large enough to be observed with electron microscopy are rhomboidal in cross-section (6, 8, 12), reflecting the unit crystal structure of the mica (15). This characteristic diamond shape is maintained up to micron-sized pores. The included angles between the equal sides of the rhombus are 60° and 120°, with slightly rounded corners. To the extent that our pore size measuring techniques were capable of revealing a pore size distribution we found, in agreement with Bean (6), that all pores in a given membrane were essentially identical. This identity of pore size contradicts the results of Beck and Schultz (8) who report a size distribution. This point is further discussed below.

Is pore size uniform at breakthrough? For 7 μ thick mica we compute a breakthrough radius of about 25 A. (The breakthrough radius is a function of membrane thickness; values from 20 to 50 A have been reported [5, 7].) From the spectrum of fragment energies which cause tracks and the penetration characteristics in mica, it is probable that for 7 μ membranes the pore size distribution remains narrow down to radii approaching the breakthrough value. Data on uniformity at breakthrough are not available.

The etching curve of r vs. t has been measured by Bean et al. (7) from breakthrough out to radii of several microns. They follow electrolyte conduction (HF) in the pore while etching is taking place. For pore radius greater than 100 A the etching rate appears to be linear. For smaller radii the growth is nonlinear, with the nonlinearity attributed to curvature effects at the pore wall. Energy considerations dictate that surface molecules are more tightly bound the smaller the pore; the corners of the rhombus are probably most difficult to etch, and they represent a larger fraction of the perimeter at smaller pore sizes.

The etching rate is very sensitive to three parameters: acid concentration, temperature, and impurities present in the etching solution. At 25° C we have measured rates of 0.60 and 1.85 A/sec for HF concentrations of 20 and 34% (weight), respectively; these values indicate a rate proportional to the square of acid concen-

tration (in agreement with Bean [7]). Price and Walker (5) observed an increase in growth rate (20% HF) by a factor of 12 on increasing temperature from 20 to 50°C, consistent with an Arrhenius energy of 16 kcal/mole. As to impurities, Peterson (18) reports that the addition of reaction products *enhances* the etching rate of fission-damaged polycarbonate by NaOH. The explanation he proposes for this curious behavior is that the products precipitate out metal ion impurities which inhibit the etching process. We experienced a case in which two solutions prepared from two different bottles of concentrated acid (same manufacturer; different lot numbers) yielded etching rates differing by a factor of *two*, although quantitative analysis showed both to contain 20% HF. A possible explanation is that the sample which produced the erratic rate contained a trace amount of inhibiting impurity (possibly one of the etching products, fluosilicic acid).

Pore Overlap

Although individual pores are uniform, there is a probability that two or more pores will overlap, and this probability increases as the fraction of membrane covered by pores increases. Because the irradiation process is random, the binomial formula can be used to estimate the number of pores (m) per square centimeter of membrane that result from a combination of q etched tracks, i.e. $q = 1$ for a single pore, 2 for a doublet, etc. The fraction of pores with q overlap is (see Appendix for derivation):

$$\frac{m(q)}{n} = \frac{(n-1)!(4\pi r^2)^{q-1}(1-4\pi r^2)^{n-q}}{q!(n-q)!},$$

$$\cong \frac{(4f)^{q-1}}{q!}\left[1 - 4f + 8f^2 - \frac{32}{3}f^3 + \cdots\right], \qquad (1)$$

where r is the radius of a single etched pore, n is the track density, and f is the total pore area fraction *if* all pores remained single ($n\pi r^2$). Thus, a membrane with an area area fraction *if* all pores remained single ($n\gamma r^2$). Thus, a membrane with an area fraction of 2% will have only 92% of the original discrete tracks remaining as single pores after etching. Note also that because of overlap the density of etched pores, $\sum_{q=1}^{\infty} m(q)$, is less than the track density since $\sum_{q=1}^{\infty} q \cdot m(q) = n$. The maximum pore area fraction is dictated by the strength of the mica; for pore areas greater than about 5% the membrane will fracture (8).

Beck (19) reports a pore size distribution for mica membranes. For one membrane a histogram is shown that indicates 90% of all pores had a radius ±26% of the mean, 63 A. These data were obtained from electron micrographs, the resolution of which is low at this small hole size. The pore area fraction of this membrane was 2.4%. Equation 1 implies that only 90% of the tracks yield single pores at this area fraction. It may be that overlap accounts in part for the reported distribu-

tion; it cannot be the total explanation, however, since overlap would appear as a distribution skewed toward larger r, the opposite of the slight skewness displayed by Beck's histogram.

Membrane Cleaning

The pore wall in the mica membranes is readily contaminated by impurities, especially organic, surface-active materials. If contaminated by organic material, the pore may be rendered nonwetting if the membrane is allowed to dry. It is advisable to keep the membrane wet for all liquid phase applications. We found chromic acid to be a satisfactory cleaning agent; it does not etch the pores (16). Various organic solvents (distilled before use) as well as hot concentrated KOH were also used in removing various impurities. In the absence of bulk flow through the membrane (which tends to plug the pores if impurities are present), pores showed no measurable change in carefully purified distilled water for periods up to 24 hr, provided the membrane was cleaned in chromic acid beforehand. Membranes can be cleaned and reused indefinitely; all instances of membrane failure resulted from fracture of the fragile mica disc. To give mechanical stability to the membrane, it can be epoxied to a heavier, supporting material; however, in all aqueous work we found that we could not totally free the system from trace impurities emanating from the epoxy. Also, the presence of epoxy limits the cleaning agents which can be used with the supported membrane.

MEASUREMENT OF PORE RADIUS

With pore length (l) and number density (n) measured independently, an absolute value for pore radius can be obtained from several different methods. We report here two accurate, straightforward techniques which have been used successfully for radius determinations down to the smallest radii obtainable. The two techniques complement each other and since one depends on gas flow and the other on electrolyte conduction, comparison of the two measurements yields an unequivocal test for the validity of each method.

Knudsen Gas Flow

If the mean free path of the permeating gas molecules is much larger than the radius of a pore, the Knudsen equation (10, 20) can be used to relate gas flux (N) to pressure difference across the membrane:

$$N = \frac{8}{3}\left[\frac{2}{\pi MRT}\right]^{1/2} n\left[\overline{\frac{A^2}{H}}\right]\Delta P\,, \qquad (2)$$

where $[\overline{A^2/H}]$ is the number-averaged value of (pore cross-section)^2/(pore wall area), M is the molecular weight of the permeating gas, R is the gas constant, and T

the absolute temperature. Accounting for the rhombic geometry of the mica pores, this equation can be rewritten in terms of r, the radius of a circle having area equal to that of the pore (i.e., the side of the rhombus is equal to $(\pi/2\sqrt{3})^{1/2} = 0.952$ times the diameter of the equivalent circle and

$$\left[\frac{\overline{A^2}}{\overline{H}}\right] = \frac{1}{4}\left(\frac{\sqrt{3}}{2}\pi^3\right)^{1/2}\frac{\overline{r^3}}{\overline{l}},$$

where $\overline{r^3}$ is the number-averaged cube of the radius):

$$N = \frac{2\pi}{3}\left[\frac{\sqrt{3}}{MRT}\right]^{1/2}\frac{n\overline{r^3}}{\overline{l}}\Delta P \equiv K\Delta P, \tag{3}$$

K is defined as the Knudsen coefficient. Measurement of K allows calculation of the root-mean-cube pore radius.

The validity of equation 3 rests on several assumptions. The principal ones are: ideal gas behavior, molecules impinging on the tube wall undergo random cosine scattering, and negligible end effects. Corrections are available to handle small deviations from these idealized conditions where the nature of the gas, its pressure, or the length-to-diameter ratio for the specific membrane does not precisely satisfy the listed assumptions (20, 21).

The apparatus used to measure the Knudsen coefficient is shown in Fig. 2. The mica membrane is epoxied to a thicker mica or stainless steel washer (this is not

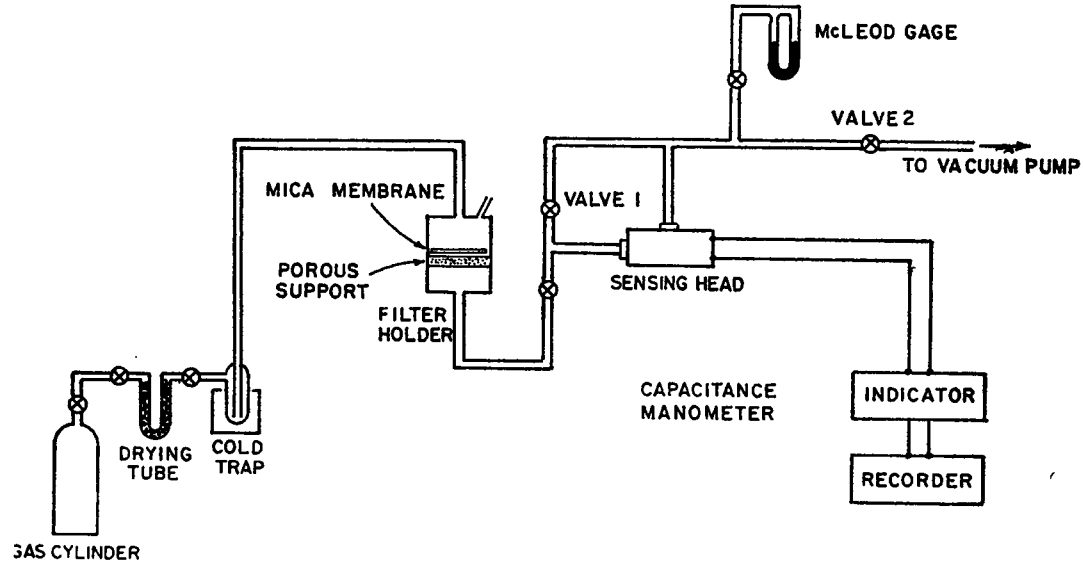

FIGURE 2 Schematic diagram of apparatus used for Knudsen flow measurements. Continuous pressure measurement is made with a Granville-Phillips (series 212, model 03) capacitance manometer (Granville-Phillips Co., Boulder, Colo.).

necessary, but it simplifies handling and sealing problems) and is placed in the pressure cell which is, essentially, a modified filter holder. An O-ring on either side of the membrane prevents leaks to the atmosphere. Pure, permeating gas is admitted to the "high" pressure side; a vacuum is drawn on the low side. At $t = 0$ the valve (number 1 in Fig. 2), on the low pressure side is closed, and the pressure of the permeating gas builds up on the low side. This pressure increase is measured with a capacitance manometer and recorded as a function of time. From these data the Knudsen coefficient can readily be calculated (10). To check the reliability of the data, four different gases (Ar, H_2, N_2, O_2) were routinely used: typical results on any one membrane agreed within 1% in K among the gases. Precautions were taken to prevent H_2O from entering the system since it is readily adsorbed on the pore walls.

Electrolyte Conduction

In the absence of concentration gradients, conduction of ions is governed by Laplace's equation for the electrical potential (22). For pores of constant cross-section and large length-to-diameter ratios, the electrical resistance across a porous mica membrane is

$$R_m = V/I = K_m/\kappa, \tag{4}$$

where V is the potential drop across the membrane, I is the total current through the membrane, κ is the specific conductivity of the solution within the pores, and K_m is the geometric cell constant

$$K_m = \frac{l}{A_0(n\pi\bar{r^2})}, \tag{5}$$

with A_0 the total irradiated area of the membrane. (Note that both here and in the gas flow measurements only the central portion of the mica disc was irradiated; the irradiated area for conductivity measurements was approximately 0.18 and 3.5 cm^2 for the gas studies.) Measurement of K_m yields the root mean square pore radius.

For finite length-to-diameter ratios an additional resistance occurs at the pore mouth because of the distortion of the current streamlines. This resistance may be expressed as an addition to the pore length and is given by (23)

$$\Delta l = 1.64\, r. \tag{6}$$

The specific conductivity of the solution within the pores is assumed to be the same as that of the bulk κ_∞ (24). For the smallest pores minor corrections must be made to allow for the hydrodynamic drag exerted by the wall on the conducting ions. These corrections are applied by combining the effects of steric hindrance and wall

drag into a single equation, with ionic radius designated by a,

$$\kappa/\kappa_\infty \cong [1 - a/r]^4. \tag{7}$$

Equation 7 is an approximate extension of the equation introduced by Pappenheimer et al. (25), and subsequently examined by Pappenheimer (26) and by Renkin (1). (It is approximate in the sense that the formula for the wall drag has been expanded, retaining only the first term in the expansion, thereby limiting equation 7 to small values of a/r.) The hydrodynamic equation used by Pappenheimer and Renkin is valid only for a particle traveling on the center line of a cylinder. If one allows for the influence of brownian motion on the position of the ion within the pore, a somewhat larger correction is predicted (16)

$$(\kappa/\kappa_\infty)_B \cong [1 - a/r]^6. \tag{8}$$

Combining equations 4, 5, 6, and 8 yields the final expression used to compute pore radius from measured membrane resistance

$$R_m = \frac{[1 + 1.64(r/l)]l}{\kappa^\infty A_0(n\pi\bar{r}^2)[1 - a/r]^6}. \tag{9}$$

Fig. 3 shows a diagram of the membrane conductivity cell and electrical circuit used to measure R_m. The mica disc is placed between two half-cells with Neoprene gaskets bearing on either side of the disc. For sealing, the thumbscrew and threaded Plexiglas rod exert a uniform compression on the gaskets and disc without subjecting the membrane to any shearing stress. This apparatus, which evolved from several preliminary designs, ensures that there is no conducting path across the membrane other than the pores by having the outer edge of the disc protrude beyond the gasket into the surrounding air. The major experimental difficulty in designing a cell with the mica disc is one of sealing the fragile disc against microscopic leaks since the resistance of the membrane is so large and sealing it without using epoxy or grease which, ultimately, introduce impurities. For temperature control the apparatus is placed inside a watertight enclosure which is submerged in a temperature bath.

After the membrane is inserted, each half-cell is filled with 0.1 M KCl. (At this ionic strength electrokinetic effects caused by the double layer at the pore wall are negligible over the entire range of etched pore radii [16].) The membrane capacitance is large ($\sim 10^{-9}$ farads); therefore the resistance measurement is most easily made using a DC current and reversible electrodes. A large resistor (R_r) loads the circuit to yield a constant current ($\pm I$) through the cell and the outer pair of Ag-AgCl wire electrodes. The current direction is changed every 10 sec to reduce electrode polarization and effects due to possible differences between anode and cathode reactions. Voltage drop ($\pm V$) across the membrane is measured with an electrometer (with DC input impedance greater than 10^{14} ohms) connected to the inner two Ag-AgCl

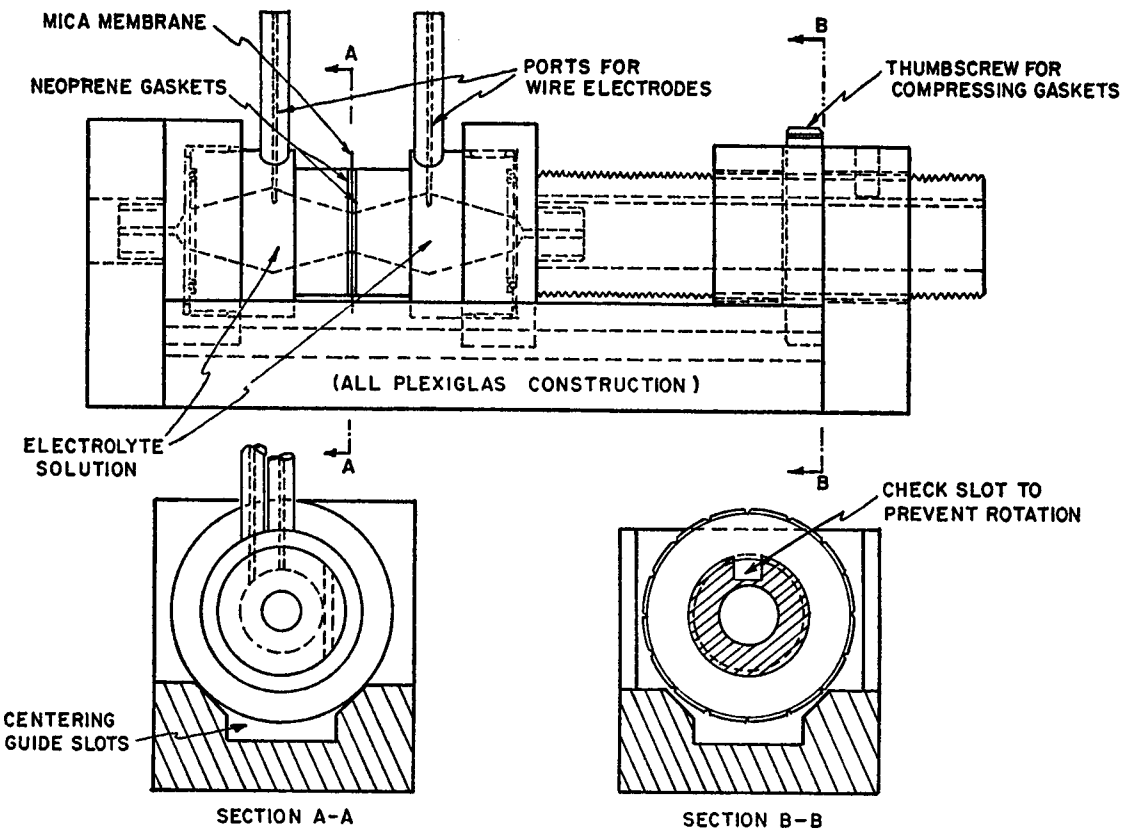

FIGURE 3 *a* Conductivity cell used in measuring electrolyte conduction in microporous mica membranes. Thumbscrew arrangement permits compression of gaskets without subjecting fragile mice sheet to shearing stresses. Two pairs of Ag-AgCl wire electrodes provide for current supply and for voltage measurement. Electrode ports are also used in adding or removing fluid from cell.

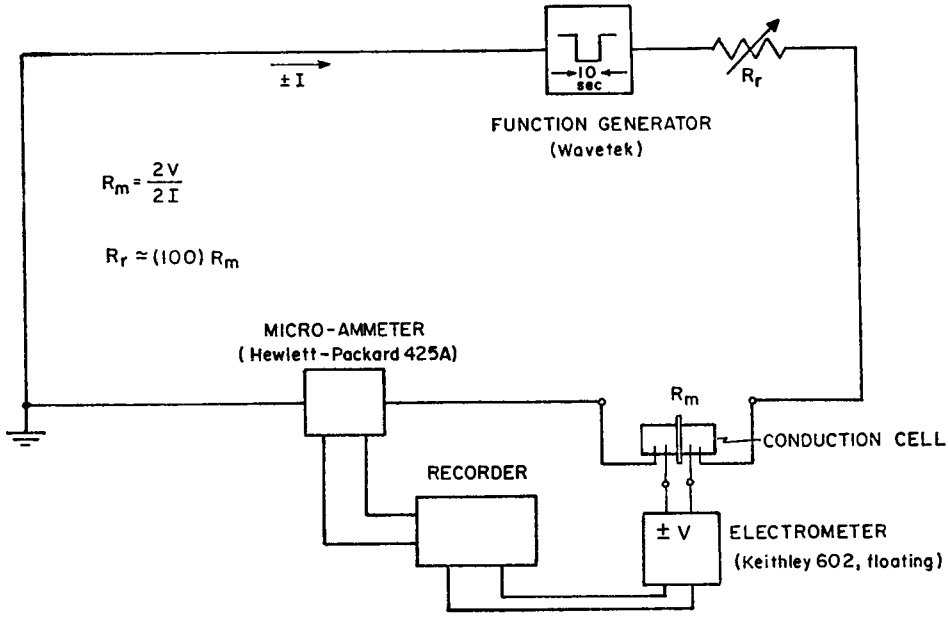

FIGURE 3 *b* Circuit for measuring membrane resistance; DC measurement with current direction changed every 10 sec. Membrane resistance is computed from peak-to-peak readings, i.e., $R_m = 2V/2I$. Pore density selected to make membrane resistance approximately 10^6 ohms in 0.1 M KCl. Function generator, Wavetek, San Diego, Calif.; microammeter, Hewlett-Packard Co., Palo Alto, Calif.; electrometer, Keithley Instruments, Inc., Cleveland, Ohio.

electrodes. Potential drop across the solution between the membrane and the voltage electrodes is entirely negligible. This double (reversible) electrode pair arrangement eliminates any influence of electrode processes on the resistance measurement. The membrane resistance is computed from the peak-to-peak readings, i.e., $R_m = 2V/2I$.

RESULTS ON PORE SIZE MEASUREMENT

Fig. 4 shows pore radius as a function of etching time as measured by the two methods described above. Each Knudsen measurement was obtained with a different membrane while seven membranes were used in the conduction data shown, some of which were reetched several times. The pore length was approximately constant for all the membranes; the pore density varied by a factor of 300.

The shape of the curve in Fig. 4 agrees with data reported by Bean et al. (7). We did not attempt to measure the breakthrough radius, but an extrapolation from our data indicates an initial pore radius of 25 A or smaller. The slope of the linear portion of the curve is 0.60 A/sec. Another etching curve (not shown) measured under similar conditions but with the 20% HF etching solution made from a different acid source (J. T. Baker Chemical Co., Tustin, Calif., vs. Fisher Scientific Co., Pittsburgh,

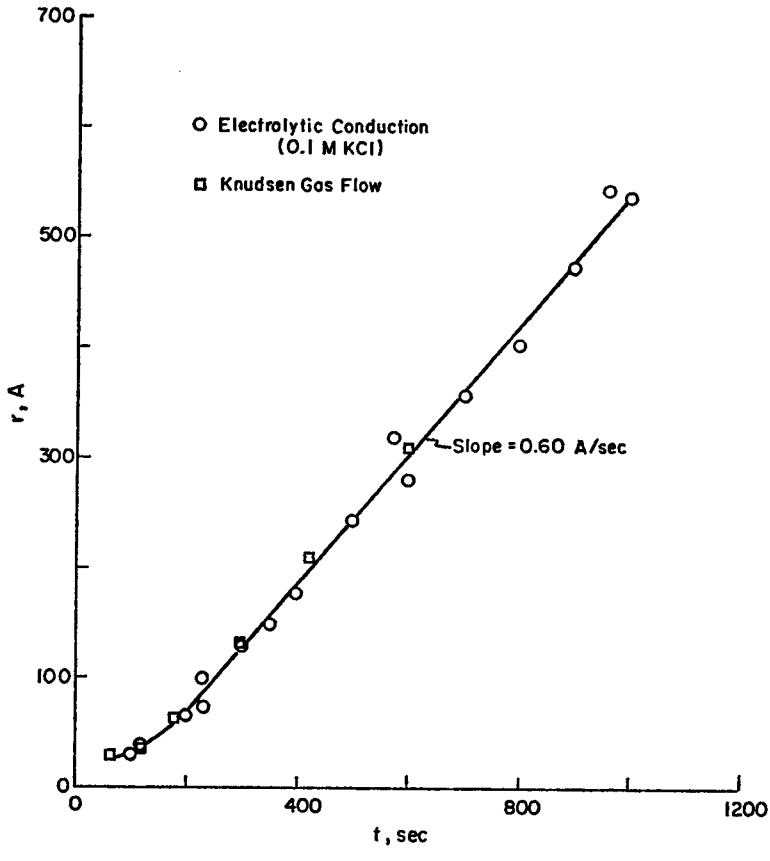

FIGURE 4 Pore radius vs. etching time for 20% HF solution at 25°C. Each Knudsen point represents a different membrane; seven different membranes were used in obtaining the electrolyte conduction data shown (some of which were reetched several times). Pore density varied between membranes. For the majority of the experiments the area occupied by pores was of the order of 10^{-5} cm^2/cm^2 of membrane. The nonlinear portion of the curve at small etching times is peculiar to the etching process near breakthrough.

Pa., for the data presented in Fig. 4) yielded a linear rate of 0.62 A/sec. Logarithmic interpolation with respect to temperature of the electron microscopy data of Price and Walker (5) shows a value of 0.56 A/sec at 25°C for a 20% HF solution. The rate for 34% HF at 25°C was found to be 1.85 A/sec by both electrolyte conduction and by visual calibration with a light microscope.

The excellent agreement between the data obtained by Knudsen gas diffusion and by electrolyte conduction warrants the following conclusions: (*a*) either method is sufficient to accurately measure pore radii; (*b*) bulk water properties (viscosity, dielectric constant) describe the aqueous phase within mica pores over the size interval shown; (*c*) agreement of the two sets of results implies that the root mean square radius equals the root mean cube radius and, therefore, the pore size distribution is narrow.

This last statement is not a strong conclusion in a statistical sense. A gaussian distribution with standard deviation of 30%, for example, gives but a 5% difference between the root mean square and root mean cube radius, a difference comparable with the precision of the data shown in Fig. 4. Stronger indications of the narrow pore size distribution are given by electron microscopy results (5) and by consideration of the damage mechanism during track formation (13, 14). Finally, the data of Fig. 4 can be used to demonstrate that the pores have negligible taper. Since the breakthrough time in 7 μ thick mica is less than 50 sec the axial etching rate must be greater than 7×10^2 A/sec, a factor of 10^3 greater than the radial rate.

COATING THE PORE WALL

Petzny and Quinn (10) described a technique for coating the pore walls of a track-etched mica membrane with molecular layers of surface-active materials. The coating is accomplished by depositing monolayers of the coating material onto the cleavage plane of an etched membrane. Deposited material migrates into the pores by surface diffusion and oriented layers form with thickness equal to that deposited on the plane. Here we present additional coating results.

The pore radius of a clean membrane was determined by Knudsen flow. Using the Langmuir-Blodgett technique either a mono- or trimolecular layer of a straight chain, fatty acid was deposited on one face of the membrane (27). After the coated membrane had dried for at least 2 hr, during which time the molecular layers presumably migrated into the pores and lined the walls, the Knudsen coefficient was again measured to determine the coated pore radius. Allowing for the fact that the radius is based on a circle of equivalent area whereas the pore is a 60° rhombus, a geometric correction factor must be used to relate the decrease in pore radius (Δr) to the coating thickness *normal* to the wall (ΔC): $\Delta C = \Delta r\,(\pi\sqrt{3}/8)^{1/2} = 0.825\,\Delta r$.

Experimental results for ΔC are shown in Tables I and II for different values of uncoated pore radius (r), number of molecular layers (one or three), and length of fatty acid chain (number of carbon atoms). The data on stearic acid show most convincingly that the pore wall was lined with a number of layers equal to that deposited onto the cleavage plane. Assuming a carbon-carbon bond length of 1.54 A (24), one would expect a monolayer of stearic acid to be somewhat less than $17 \times 1.54 = 26$ A since tetrahedral bonding would prevent full perpendicular extension of the bonds from the interface. The literature value for the thickness of a stearate layer on a flat surface is 24 A (28). The thickness values of Tables I and II may be slightly less than the actual values since the corners of the rhombus-shaped pore may be accessible to the permeating gas molecules but not to the fatty acid coating. From Table II the average increase in layer thickness per carbon atom in the homologous series of deposited straight-chain acids is about 1.6 A, in agreement with the carbon-carbon bond length.

Wall coatings are not limited to fatty acids. Preliminary data on monolayers of

TABLE I

STEARATE LAYERS DEPOSITED ON MICA: LAYER THICKNESS NORMAL TO PORE WALL

Pore radius before coating	Number of layers deposited on cleavage plane	ΔC	ΔC/layer
A		*A*	*A*
110	1	21	21
140	1	21	21
140	3	61	20
165	1	22	22
180	1	23	23
200	1	23	23
234	3	67	22
240	1	22	22
240	3	67	22

TABLE II

A SERIES OF FATTY ACID MONOLAYERS DEPOSITED ON MICA: LAYER THICKNESS NORMAL TO PORE WALL

Fatty acid	Pore radius before coating	ΔC*
	A	*A*
Palmitic (C_{16})	180	21
Stearic (C_{18})	180	23
	200	23
Arachidic (C_{20})	180	29
	200	26
Behenic (C_{22})	180	32
	200	29
Lignoceric (C_{24})	180	34

* Average *increase* in layer thickness per carbon atom = 1.6 A.

α-dipalmitoyl lecithin deposited under a nitrogen atmosphere give Δr of 29 A, equivalent to a wall coating 24 A thick.

Application of the coating technique to aqueous systems introduces some problems. The coated membrane on drying becomes nonwetting because the pore wall presents a hydrophobic surface. To overcome this problem the coated membrane

was first contacted with an ethanol solution which did wet the pores. The ethanol was then removed from the solution by dilution with pure water. This procedure gave a coating thickness of 39 A for a stearate bilayer in a 182 A pore (determined by electrolyte conduction). Unfortunately, ethanol was found to dissolve some of the coated layer, introducing an unknown factor into the results. A better approach to deposition may be direct adsorption from a solution of the surface-active material, a technique which has been used to build up layers on flat surfaces (29). Limited data on adsorption of the protein bovine serum albumin from dilute solution showed that the protein adsorbed strongly but, possibly, not in a uniform layer (16).

We thank C. P. Bean of the General Electric Research Laboratories for supplying information on various aspects of the fabrication and calibration techniques.

This work was supported in part by a grant from the Office of Saline Water, U. S. Department of the Interior and by a grant from the American Oil Company.
J. L. Anderson was the recipient of a National Institutes of Health Research Fellowship.

Received for publication 3 January 1972.

APPENDIX

Prediction of the Extent of Pore Overlap

Consider a 1 cm^2 area of the membrane as a basis. The total number of impinging fission fragments is n, and r is the etched radius of a discrete pore. Because the overlap occurs when the individual damaged tracks are etched and "grow" into each other, construct a model which assumes a random distribution of fully etched, circular pores of radius r covering the face of the membrane. The randomness of the irradiation ensures that

$$\begin{aligned} p &= 4 \cdot (\text{area of one pore}), \\ &= 4\pi r^2 , \end{aligned} \qquad (A\,1)$$

where p is the probability that any given pore will overlap with (touch) another single, specified pore whose position is fixed within the membrane.

Consider that pore which is the first to be located on the membrane. The probability $P(w)$ that just w other pores will overlap with this initial one is given by the binomial distribution:

$$P(w) = \frac{(n-1)!}{(n-1-w)!} p^w (1-p)^{n-1-w}. \qquad (A\,2)$$

Any of the pores may be chosen as the initial pore, so that the right hand side of equation A 2 must be multiplied by n; however, $(w+1)!$ should be divided into equation A 2 to arrive at overlap combinations, not permutations. The resulting expression is

$$\frac{m(q)}{n} = \frac{(n-1)!\,p^{q-1}(1-p)^{n-q}}{q!(n-q)!}, \qquad (A\,3)$$

where $m(q)$ is the number of pores that consist of q overlapping single pores (i.e., $q = 1$ implies a single, $q = 2$ a doublet, etc.), $q = w + 1$. Because $n \sim 10^4 - 10^8 \gg q$, equation A 3 may be simplified to

$$\frac{m(q)}{n} = \frac{(np)^{q-1}(1-p)^n}{q!}. \qquad (A\ 4)$$

By expanding the above and invoking relation A 1 the desired expression for estimating the extent of overlap obtains:

$$\frac{m(q)}{n} = \frac{(4f)^{q-1}}{q!}\left[1 - 4f + 8f^2 - \frac{32}{3}f^3 + \cdots\right] \qquad (A\ 5)$$

where $f = n\pi r^2$, the pore area fraction of the membrane that would exist if all pores remained discrete. It follows directly that $\sum_{q=1}^{\infty} q \cdot m(q) = n$.

It should be mentioned that the above analysis is not exact since p changes slightly with w (or q) due to a small increase in the target area of the multiple overlaps. The error resulting from neglecting this change should be unimportant [at least in computing $m(1)$ and $m(2)$] because very few combinations of three or more single pores are expected. Microscopic observations have verified this speculation.

REFERENCES

1. RENKIN, E. M. 1954. *J. Gen. Physiol.* **38**:225.
2. SOLOMON, A. K. 1968. *J. Gen. Physiol. Suppl.* **51**:335 s.
3. BEAN, C. P. 1972. The Physics of Porous Membranes, I. *In* Membranes—A Series of Advances, Vol. 1. G. Eisenman, editor. Marcel Dekker, Inc., New York. In press.
4. PRICE, P. B., and R. M. WALKER. 1962. *J. Appl. Phys.* **33**:3400.
5. PRICE, P. B., and R. M. Walker. 1962. *J. Appl. Phys.* **33**:3407.
6. BEAN, C. P. 1969. Characterization of Cellulose Acetate Membranes and Ultrathin Films for Reverse Osmosis. Office of Saline Water, Research and Development Progress Report No. 465.
7. BEAN, C. P., M. V. DOYLE, and G. ENTINE. 1970. *J. Appl. Phys.* **41**:1454.
8. BECK, R. E., and J. S. SCHULTZ. 1970. *Science (Wash. D. C.).* **170**:1302.
9. ANDERSON, J. L., and J. A. QUINN. 1972. *Faraday Soc. Trans.* **68**:608.
10. PETZNY, W. J., and J. A. QUINN. 1969. *Science (Wash. D. C.).* **166**:751.
11. FLEISCHER, R. L., and P. B. PRICE. 1964. *J. Geophys. Res.* **69**:331.
12. FLEISCHER, R. L., P. B. PRICE, and R. M. WALKER. 1963. *Rev. Sci. Instrum.* **34**:510.
13. FLEISCHER, R. L., P. B. PRICE, and R. M. WALKER. 1965. *Science (Wash. D. C.).* **149**:383.
14. FLEISCHER, R. L., P. B. PRICE, and R. M. WALKER. 1969. *Sci. Am.* **220**(6):30.
15. DEER, W. A., R. A. HOWIE, and J. ZUSSMAN. 1966. *In* An Introduction to the Rock Forming Minerals. John Wiley and Sons, Inc., New York. 193–205.
16. ANDERSON, J. L. 1971. Characterization of mass and charge transport: development of a model membrane. Ph.D. Thesis. University of Illinois, Urbana.
17. Friedlander, G., J. W. Kennedy, and J. M. Miller. 1964. *In* Nuclear and Radiochemistry. John Wiley and Sons, Inc., New York. 2nd edition. 565.
18. Peterson, D. D. 1970. *Rev. Sci. Instrum.* **41**:1252.
19. BECK, R. E. 1969. Restricted diffusion of nonelectrolytes through artificial mica membranes with known pore geometry. Ph.D. Thesis. University of Michigan, Ann Arbor.
20. DUSHMAN, S. 1962. Scientific Foundations of Vacuum Technique. John Wiley and Sons, Inc., New York. 2nd edition.
21. HO, W. S. 1971. Model membranes: Knudsen flow through microcapillaries. Ph.D. Thesis. University of Illinois, Urbana.

22. NEWMAN, J. 1967. *Adv. Electrochem. Electrochem. Eng.* **5**:87.
23. NANIS, L., and W. KESSELMAN. 1971. *J. Electrochem. Soc.* **118**:454.
24. HODGMAN, C. D., editor. 1962. Handbook of Chemistry and Physics. The Chemical Rubber Co., Cleveland, Ohio. 44th edition.
25. PAPPENHEIMER, J. R., E. M. RENKIN, and L. M. BORRERO. 1951. *Am. J. Physiol.* **167**:13.
26. PAPPENHEIMER, J. R. 1953. *Physiol. Rev.* **33**:387.
27. BLODGETT, K. 1935. *J. Am. Chem. Soc.* **57**:1007.
28. GAINES, G. L., JR. 1966. *In* Insoluble Monolayers at Liquid-Gas Interfaces. Interscience Publishers Inc., New York. 339.
29. ADAMSON, A. W. 1967. *In* Physical Chemistry Surfaces. Interscience Publishers Inc., New York. 2nd edition. 397.